INTERNATIONAL JOURNAL OF REFRIGERATION 55 (2015) 212–223

Available online at www.sciencedirect.com

ScienceDirect

journal homepage: www.elsevier.com/locate/ijrefrig

Investigation of an experimental ejector refrigeration machine operating with refrigerant R245fa at design and off-design working conditions. Part 2. Theoretical and experimental results

K.O. Shestopalov [a,b,*], B.J. Huang [a], V.O. Petrenko [a,b], O.S. Volovyk [a]

[a] New Energy Center, Department of Mechanical Engineering, National Taiwan University, Taipei 106, Taiwan
[b] Odessa State Academy of Refrigeration, Ejector Refrigeration Technology Center, 1/3, Dvoryanskaya St., 65082 Odessa, Ukraine

ARTICLE INFO

Article history:
Received 15 November 2013
Received in revised form
29 December 2014
Accepted 9 February 2015
Available online 19 February 2015

Keywords:
Ejector
Ejector refrigeration machine
R245fa
Test rig
Performance characteristics

ABSTRACT

The main results of a theoretical and experimental investigation of the performance characteristics of an ejector and an ejector refrigeration machine (ERM) operating with refrigerant R245fa at design and off-design working conditions are presented. The ejector and ERM were explored theoretically using improved 1D model and the calculated results were validated experimentally on ejector test rig that has been assembled and operated at National Taiwan University. For typical cases, the performance characteristics variation with condensing, generating and evaporating temperatures along with performance maps are presented. The theoretical results are compared with the results of a set of experiments and good qualitative and quantitative agreement is observed.

Une étude du fonctionnement d'un système frigorifique expérimental de réfrigération à éjecteur avec le frigorigène R245fa aux conditions de travail de conception et hors-conception. 2ème partie -Résultats théoriques et expérimentaux

Mots clés : Ejecteur ; Machine frigorifique à éjecteur ; R245fa ; Banc d'essai ; Caractéristiques de performance

* *Corresponding author*. New Energy Center, Department of Mechanical Engineering, National Taiwan University, Taipei 106, Taiwan. Tel.: +886 2 23634790.
E-mail address: konalex2@yandex.ru (K.O. Shestopalov).
http://dx.doi.org/10.1016/j.ijrefrig.2015.02.004
0140-7007/

Nomenclature

1, 2, 3	number of nozzle (Fig. 6)
1, 2, 3	number of conical-cylindrical mixing chamber (Fig. 8)
A, B, C	number of cylindrical mixing chamber (Fig. 7)
A	area (mm^2)
COP	coefficient of performance
d	diameter (mm)
ERM	ejector refrigeration machine
h	specific enthalpy (kJ kg^{-1})
k	thermal conductivity (W m^{-1} K^{-1})
l	length (mm)
$\dot{m}$	mass flow rate (kg s^{-1})
P	pressure (bar)
Q	heat flow (kW)
q	specific heat of evaporation (kJ kg^{-1})
T	temperature (°C or K)
$\dot{W}$	power (kW)

Greek letters

β	ejector area ratio
ψ	angle
ω	entrainment ratio
υ	flow coefficient

Subscripts

actual	actual
b	boiling
c	condenser
cr	critical
e	evaporator
fp	feed pump
g	generator
mech	mechanical
max	maximum
n	nozzle
p	primary
s	secondary
sub	subcooling
suc	suction
t	throat
therm	thermal
1, 2, 3, 4	cross-sections of the ejector (Tables 1, 2 and 4)
1, 2, 3…11	measuring points of temperature (Fig. 3)

1. Introduction

The ejector refrigeration machine (ERM) offers several advantages over the other heat-driven refrigeration cycles, including simplicity in design and operation, high reliability and low installation cost, which enable their wide application in the production of cooling (Petrenko et al., 2011).

In Part 1 of this paper (Shestopalov et al., 2015) an improved 1-D mathematical model for determination of the entrainment ratio ω and optimal design of ejectors with cylindrical mixing chamber (CMC) and conical-cylindrical mixing chamber (CCMC) are proposed.

Based on theoretical comparative analysis of ejector and ejector refrigeration cycle performance characteristics for eight low-pressure refrigerants, the refrigerant R245fa was selected as the most suitable working fluid for general purpose applications in the present study.

This paper provides the main results of joint research and development carried out in the period from 2008 to 2012 at New Energy Center of the Mechanical Engineering Department, National Taiwan University, Taipei, Taiwan, in cooperation with the Odessa State Academy of Refrigeration, Ukraine, in the area of ejector refrigerating technologies that was based on the Global Research Partnership Award (GRP Award), granted by the King Abdullah University of Science and Technology (KAUST).

The ejector with advanced construction and improved flow profile and the design of ejector test rig are described in this paper. The testing technique of the experimental investigation of ERM with maximum cooling capacity of 12 kW operating at design and off-design conditions is presented.

Performance characteristics of ERM are determined; the influence of the ejector geometry and operating conditions on machine performance and characteristics is shown. The comparison of experimental and theoretical data for ERM operating at design and off-design working conditions is presented. The validation of the mathematical modeling presented in the Part 1 is done.

2. Description of experimental setup

The main components of experimental ejector refrigeration cycle include an ejector, a generator, an evaporator, a condenser, a receiver-subcooler, an expansion valve and a feed pump. The arrangement of these components is given in simplified diagram of experimental ERM (Fig. 1). The process

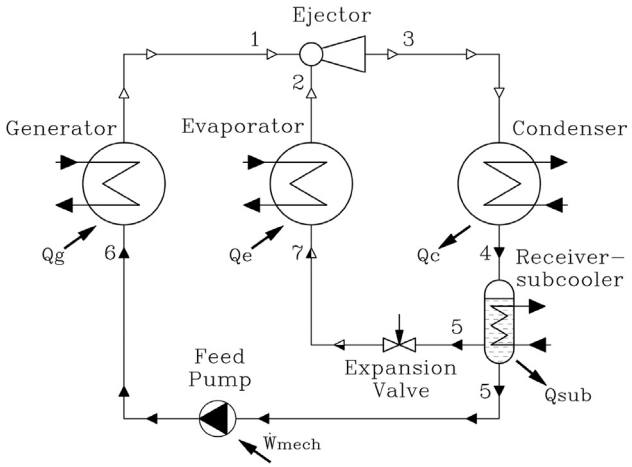

Fig. 1 – Diagram of experimental ejector refrigeration machine.

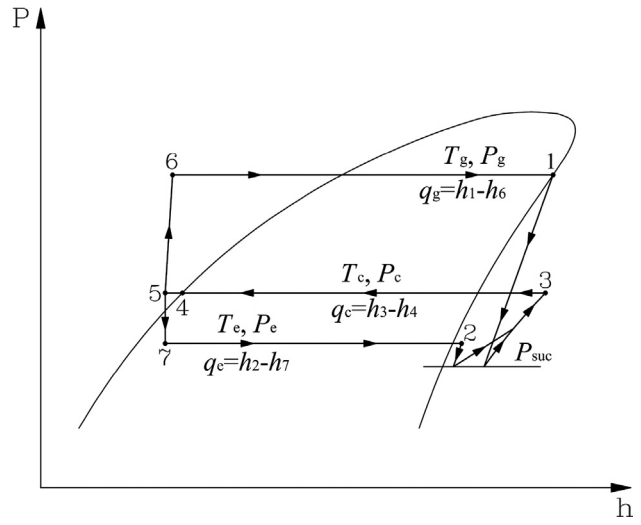

Fig. 2 – Diagram of the actual ejector refrigeration cycle.

of a continuously operating ERM is characterized by points 1–7 in Fig. 2, which is a diagram of an actual ejector refrigeration cycle of this machine.

Usually the working fluid transported through the feed pump is close to the saturation conditions. Therefore a slight drop in the condensing pressure and pump inlet pressure may therefore cause cavitation, which in turn causes loss of pump work, decreasing in the coefficient of efficiency and steady operation of the system disorder. In order to increase the dependability and effectiveness of the system as a whole it is necessary to provide sufficient subcooling of suction liquid refrigerant.

In order to improve the system performance, special receiver-subcooler is added to the cycle as it is shown in Fig. 1. The purpose of this component is to subcool the condensate prior to entering the feed pump and evaporator, thus increasing the operational reliability, specific cooling capacity q_e and effectiveness of the ejector system.

To verify the theoretical analysis of the ejector geometry and performance characteristics of the ERM using refrigerant R245fa, an ejector test rig with a cooling capacity of 12 kW was designed and constructed. A schematic diagram and a photograph of the ejector test rig are shown in Figs. 3 and 4, respectively. The ejector test rig equipment includes the following nine major components: an experimental ejector, a generator, an evaporator, a condenser, a receiver-subcooler, a float regulating valve, a gear-type feed pump, a cooling tower and a control panel equipped with different measurement instrumentation. Locations of measurement points around the circuit are shown in Fig. 3.

Fig. 5 illustrates the structure of the ejectors with cylindrical (a) and conical-cylindrical (b) mixing chambers. A cone angle of the divergent part of the supersonic nozzles was $\Psi_1 = 6°$; a cone angle of the convergent part of the supersonic nozzles was $\Psi_2 = 30°$; the angle of the entering part of the conical-cylindrical mixing chambers was $\Psi_3 = 2°$ and of the diffuser – $\Psi_4 = 8°$. The length of the mixing chamber l_{mch} was $6...10d_3$, and the length of the diffuser l_d was $10...12d_3$. Such values of the cone sections angles and lengths of the ejector flow profile confirmed the high efficiency of the previously studied ejectors operated with refrigerants R141b, R142b, R236fa и R245fa (Petrenko, 1978; Huang et al., 1999; Eames et al., 2007, 2004).

A photograph of the experimental ejector assembly with two retrofract symmetrical suction inlet ducts and a suction manifold is shown in Fig. 6. The assembly of the ejector consists of the following main components: a body, an axially movable supersonic nozzle, a mixing chamber made jointly with the diffuser, a frame and a mechanism to move the nozzle into optimal position with respect to the entrance of the mixing chamber. The ejector assembly is 510 mm in length, 60 mm in height and 130 mm in width.

The generator was designed with a cylindrical shape and had a glass level gauge for liquid level observation. The working fluid in the generator was heated by two 13 kW electric heaters those were separately controlled, as were the heat load, generating temperature and pressure. The evaporator was also designed in a cylinder shape with a glass level gauge for liquid level observation. Heat energy was directly transferred to the evaporator by two 6 kW electric heaters to simulate the evaporator cooling load. The electric heaters were also separately controlled, as were the cooling load, evaporating temperature and pressure. Electric energy inputs to the generator and evaporator were measured by electrical power meters. The generator and evaporator and all of their connecting lines were thoroughly thermally insulated. The condenser was a conventional shell-and-tube heat exchanger with a glass level gauge, cooled by water supplied from the cooling tower, with a rejected heat capacity of 52 kW. The condenser temperature and the ejector backpressure were automatically controlled by varying the water flow through the condenser. The receiver-subcooler was a specially designed shell-and-coil type vertical vessel cooled by water taken from the cooling tower. It was equipped with a level gauge and level transmitter for liquid level observation and control. The receiver-subcooler and all of its connecting lines were thermally insulated. A hydraulic gear-type pump driven by a three-phased variable speed electric motor was used as the generator feed pump.

The receiver-subcooler was equipped with level regulator (RLR) with electromagnetic level sensor. The signal from the electromagnetic level sensor was used for the automatic change of the motor speed of the feed pump by means of the inverter type regulator. Such a way the autocontrol of the output capacity of the feed pump was realized. This ensured a reliable operation of the test rig and a steady maintenance of the generator operation as well as generating temperatures and pressures. Likewise the receiver-subcooler provided a positive suction head for the regular pump operation by subcooling of the liquid refrigerant and by geometrical static suction head.

In order to carry out experimental investigations in wide range of operating conditions $T_g = 80–105$ °C, $T_c = 24–42$ °C, $T_e = 4–20$ °C and to obtain the values of $COP_{therm} > 0.4$, three supersonic nozzles №1, №2, №3 and three cylindrical mixing chambers A, B, C were designed and manufactured. Photographs of the tested supersonic nozzles and cylindrical mixing chambers made jointly with the diffusers are shown in Fig. 7 and Fig. 8, respectively. The specifications of the tested

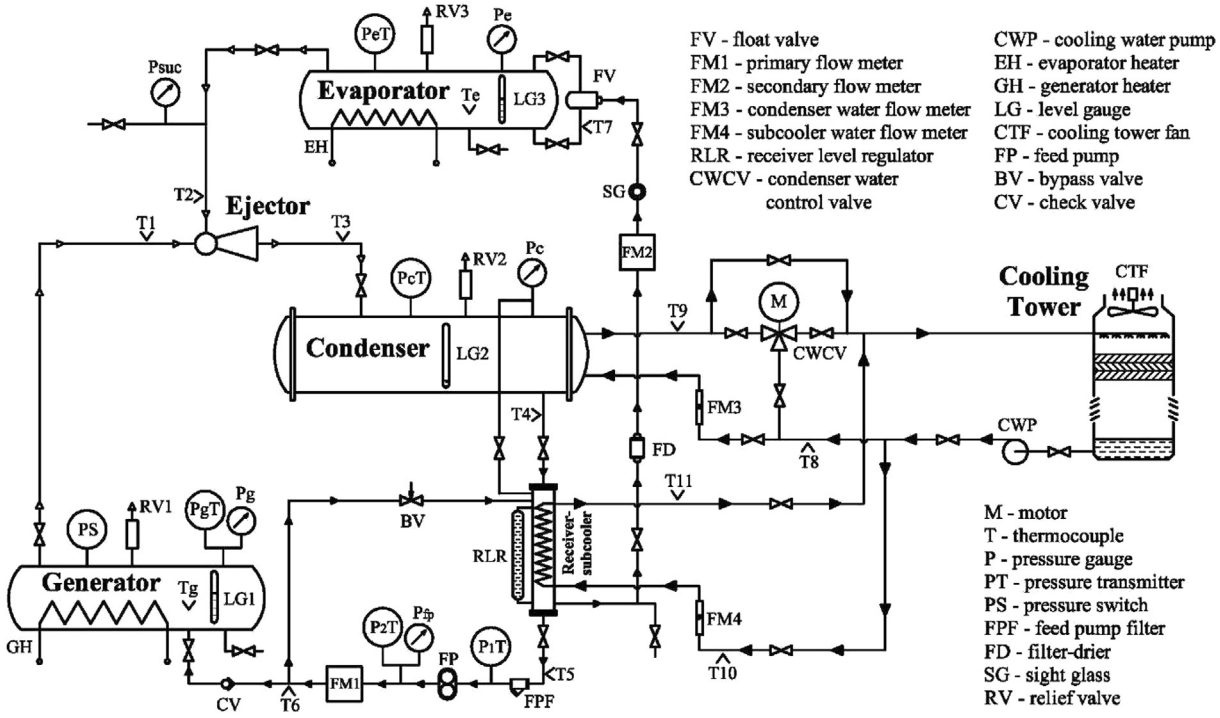

Fig. 3 – Schematic diagram of the ejector test rig.

supersonic nozzles and cylindrical mixing chambers are listed in Tables 1 and 2, respectively.

Table 3 illustrates ejector specifications obtained by combination of tested three nozzles №1, №2 and №3 and tested three constant-area mixing chambers A, B and C.

Petrenko et al., 2011 stated that the application of conical-cylindrical mixing chambers at the same operating conditions allows for improvement up to 25–35% in ω compared with cylindrical mixing chambers. In Part 1 of the present series (Shestopalov et al., 2015) it has been shown theoretically that for different low-pressure refrigerants, this improvement is in the range from 0.7% to 23.6%. For refrigerant R245fa theoretical increase in ω for ejectors with conical-cylindrical mixing chambers is 19.6% for design conditions of T_g = 95 °C, T_c = 32 °C and T_e = 12 °C.

In order to compare the performance of ejectors for R245fa using cylindrical mixing chambers with ejectors using conical-cylindrical mixing chambers, three conical-cylindrical mixing chambers 1, 2 and 3 were designed and manufactured to carry out the experimental investigations at the same operating conditions as was mentioned before and to obtain the values of $COP_{therm} > 0.6$. These new mixing chambers were

Fig. 4 – Photograph of the ejector test rig.

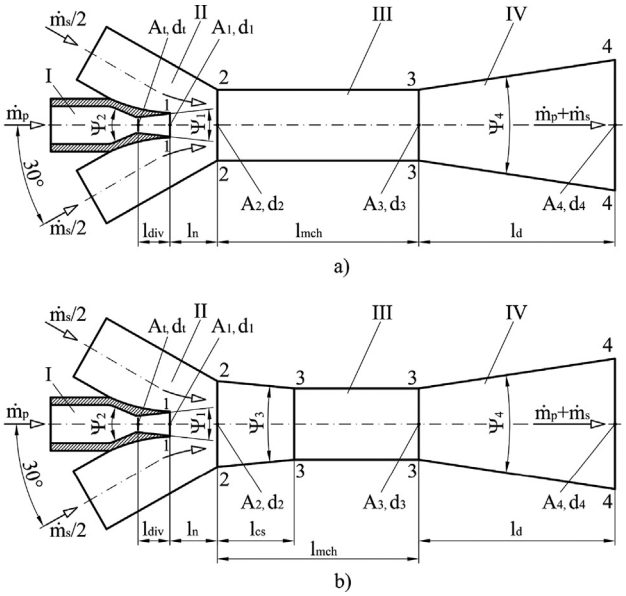

Fig. 5 – Structure of advanced ejector with cylindrical (a) and conical-cylindrical (b) mixing chambers.

Fig. 6 – Photograph of the ejector assembly.

made from cylindrical mixing chambers by boring the front part of the constant area section. Using this technology, all the dimensions of the new mixing chambers 1, 2 and 3 were the same compared to previous mixing chambers A, B and C. Only new conical section was created, which occupied part of the cylindrical section. Photograph of the manufactured conical-cylindrical mixing chambers made jointly with the diffusers is shown in Fig. 9. Additional dimensions of new mixing chambers are listed in Table 4.

3. Testing technique

A standard procedure was used for operation of the test bench. Before each test run, refrigerant liquid levels within the generator, evaporator and receiver-subcooler vessels were set to predetermine values. After replacement of the nozzle or mixing chamber, a vacuum pump was used to evacuate the air from the suction line. For each test run, the generator heaters were switched on and set to the desired generating temperature and generator heat load input. The flows of cooling water through the condenser and receiver-subcooler were adjusted by appropriate shut-off water valves and during the tests the cooling water flows were varied depending on the operating conditions. When the desired temperature in the generator was reached, the shut-off valves on primary flow line and secondary flow line were opened, and in the same time the feed pump and evaporator heaters were switched on. The pressure within the condenser (the back-pressure of the ejector) was controlled by automatic or manual adjusting the flow rate of cooling water through the condenser, and the pressures at the generator and evaporator were controlled by automatic or manual adjusting of power consumption of appropriate electric heaters.

Primary and secondary flow rates were measured by gear-type flow meters. The pressures of the primary and secondary flows, the back pressure at the condenser and the pressure after feed pump were measured using industrial direct-reading pressure gauges and pressure transmitters. Suction and condensing pressures were measured using high-precision Bourdon-tube gauges. Several K-type thermocouples were installed at appropriate places (T_1-T_{11}) for temperature measurement. RTD sensors were used to control the generating, evaporating and condensing temperatures. The

Fig. 7 – Photograph of the tested supersonic nozzles 1, 2 and 3.

generator, evaporator and condenser were protected by pressure relief valves. The flow rates of the cooling water circulating through the condenser and receiver-subcooler were measured by glass flow meters. A control panel equipped with different instrumentation and other various standard components of the refrigeration machine were also used in the construction of the ejector test rig. Specifications of the main measurement instrumentation of the ejector test rig are given in Table 5.

A PC-based monitoring and control system was developed in the present study for the ejector test rig. The data were sampled by a data acquisition system every 10 s. Pressures, temperatures, primary and secondary flow rates, electric power consumption and other required data were recorded and the results were calculated. This enabled the main performance to be determined in a steady state condition of system operation.

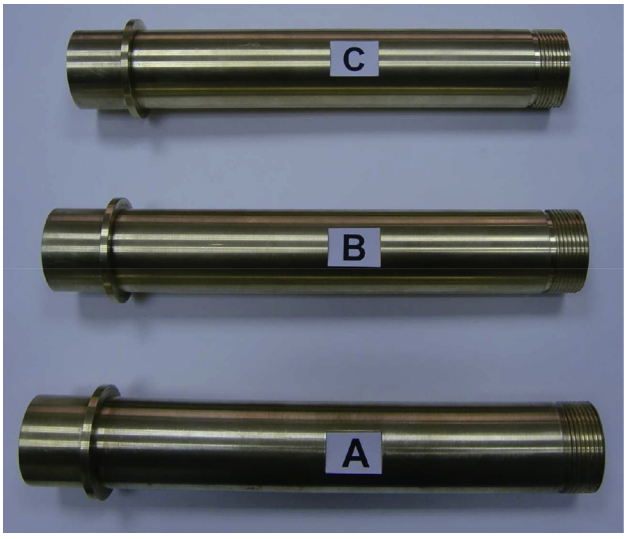

Fig. 8 – Photograph of the tested cylindrical mixing chambers A, B and C.

Table 1 – Specifications of the tested supersonic nozzles.

Number of the primary nozzle	№1	№2	№3
Operating conditions	$T_e = 8\ ^\circ C$, $T_g = 90\ ^\circ C$	$T_e = 12\ ^\circ C$, $T_g = 95\ ^\circ C$	$T_e = 16\ ^\circ C$, $T_g = 100\ ^\circ C$
Throat diameter d_t, mm	4.515	4.212	3.902
Throat area A_t, mm^2	16.0	13.93	11.95
Exit diameter d_1, mm	7.8	7.11	6.412
Exit area A_1, mm^2	47.76	39.68	32.27
Area ratio A_1/A_t	2.985	2.85	2.70
Diverging angle at nozzle exit ψ_1, deg	6.0	6.0	6.0
Converging angle at nozzle enter ψ_2, deg	30	30	30
Diverging part length l_{div}, mm	31.48	28.33	24.71

Table 2 – Specifications of the tested cylindrical mixing chambers.

Number of the cylindrical mixing chamber	A	B	C
Constant area section diameter d_3, mm	12.155	13.020	14.010
Constant section area A_3, mm^2	115.98	133.07	154.08
Length of constant area mixing chamber l_{mch}, mm	90.62	98.64	106.65
Length of diffuser l_d, mm	142.9	135.75	128.65
Diverging angle of diffuser ψ_4, deg	8.0	8.0	8.0
Exit diameter of diffuser d_4, mm	32.0	32.0	32.0
Exit area of diffuser A_4, mm^2	803.84	803.84	803.84

During experiments the value of subcooling of liquid refrigerant in suction pipeline before feed pump was 2–4 °C, the superheating of entrained vapor in suction pipeline of the ejector was 5–7 °C.

For each ejector geometry, an independent nozzle exit position test was carried out. The optimal nozzle position, which provides the maximum ejector performance, was used to test each ejector under design and off-design operating conditions. For each series of tests for design and off-design operating conditions, only one parameter of the system was varied whilst keeping the others constant in order to determine its influence on the system performance. When the ejector cooling system was operating in steady-state conditions for about 30–40 min, the pressures, temperatures, flow rates, and other required data were recorded and results were calculated. For each test the critical condensing temperature also was established and determined.

The entrainment ratio ω was determined from Eq. (1):

$$\omega = \frac{\dot{m}_s}{\dot{m}_P} \tag{1}$$

Primary and secondary flow rates were determined in two independent ways: directly (from the readings of the flow meters), and indirectly (from energy balance of generator and evaporator) from Eqs. 2–3:

$$\dot{m}_P = \frac{\dot{W}_g}{h_1 - h_6} = \frac{\dot{W}_g}{q_g} \tag{2}$$

Table 3 – Specifications of tested ejectors with constant-area mixing chambers.

Nozzles and mixing chambers combinations	A_3/A_t
Nozzle №1 – mixing chamber A (Ejector 1-A)	7.25
Nozzle №1 – mixing chamber B (Ejector 1-B)	8.32
Nozzle №1 – mixing chamber C (Ejector 1-C)	9.63
Nozzle №2 – mixing chamber A (Ejector 2-A)	8.33
Nozzle №2 – mixing chamber B (Ejector 2-B)	9.55
Nozzle №2 – mixing chamber C (Ejector 2-C)	11.06
Nozzle №3 – mixing chamber A (Ejector 3-A)	9.71
Nozzle №3 – mixing chamber B (Ejector 3-B)	11.14
Nozzle №3 – mixing chamber C (Ejector 3-C)	12.89

Fig. 9 – Photograph of the tested conical-cylindrical mixing chambers 1, 2 and 3.

Table 4 – Specification of conical-cylindrical mixing chambers.

Number of the conical-cylindrical mixing chamber	1	2	3
Conical section entry diameter d_2, mm	13.848	14.835	15.954
Area ratio $\beta = A_2/A_3$	1.3	1.3	1.3
Entry conical section angle ψ_3, deg	2	2	2
Length of mixing chamber conical section l_{cs}, mm	48.85	52.14	55.86

$$\dot{m}_s = \frac{\dot{W}_e}{h_2 - h_7} = \frac{\dot{W}_e}{q_e}. \quad (3)$$

Cooling capacity of ERM without respect to the heat gains and losses was defined according to the power consumption of evaporator heaters, i.e. $Q_e = \dot{W}_e$, and also from Eq. (4):

$$Q_e = \dot{m}_s \cdot (h_2 - h_7) = \dot{m}_s \cdot q_e. \quad (4)$$

Generator heat load without respect to the heat loss was determined by power consumption of generator heaters, i.e. $Q_g = \dot{W}_g$, and also from Eq. (5):

$$Q_g = \dot{m}_p \cdot (h_1 - h_6) = \dot{m}_p \cdot q_g. \quad (5)$$

COP_{therm} was calculated from Eq. (6):

$$COP_{therm} = \frac{Q_e}{Q_g} = \frac{\dot{W}_e}{\dot{W}_g}. \quad (6)$$

Actual power consumed by feed pump $\dot{W}_{fp}^{actual}$, was determined from direct measurement of power meter, which was inbuilt in variable speed driver. The values of $\dot{W}_{fp}^{actual}$ from experiment were used to calculate COP_{mech} from Eq. (7):

$$COP_{mech} = \frac{Q_e}{\dot{W}_{fp}^{actual}} \quad (7)$$

The material of isulation for the generator was high efficient Flexible Rock Wool (Fibertex R120) with $k = 0.036$ W m^{-1} K^{-1} and the thickness of 50 mm. The generating temperatures of refrigerant were 50–90 °C higher than ambient temperature (depending from operating conditions). Therefore, average unwanted generator heat loss was assumed to be 5% of the electrical power input. The heat loss was calculated for the maximum generator heat load and maximum temperature difference between generating and ambient temperatures this respect to the thickness and thermal conductivity of the isolating material. Hence, the generator heat load Q_g from Eq. (5) was 5% lower than measured power consumption of generator heaters $\dot{W}$.

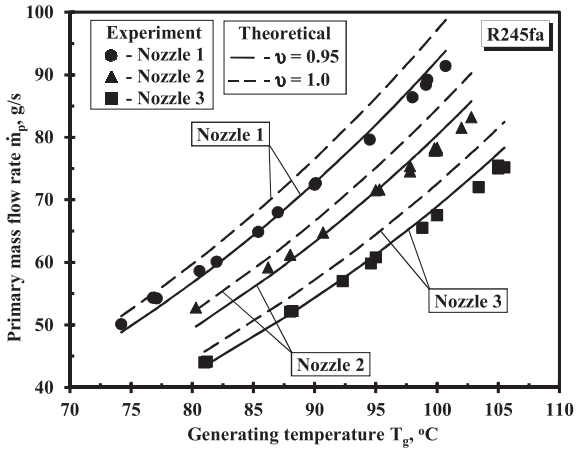

Fig. 10 – Theoretical and experimental mass flow rates of the primary nozzles 1, 2 and 3 against the generating temperature.

The evaporator was isolated with economical Flame retarded NBR/PVC polymeric foam (K-FLEX ST) with $k = 0.033$ W m^{-1} K^{-1} with the thickness of 50 mm. The evaporating temperatures of refrigerant were 10–15 °C lower than ambient temperature and sometimes even slightly higher. Thus, heat gains or losses in evaporator were negligible. Therefore, cooling capacity Q_e from Eq. (4) was the measured heat load of evaporator heaters.

During the tests, the two main errors are first of all from temperature, pressure, flow rate and heat load measurement accuracy, and secondly – from data logging and reading by the computer. A detailed error analysis indicates that the maximum uncertainty in the performance parameters is less than ±5.0%. Therefore, these errors are acceptable for the present study.

4. Experimental results and discussion

4.1. *Nozzles calibration*

The first task of the experiments that used R245fa was to calibrate the supersonic nozzles under different generating temperatures and pressures (Fig. 10). In these tests, the rig was run with a closed suction line. The calibration tests for the

Table 5 – Specifications of the measurement instrumentation of the ejector test rig.

Parameters	Instruments	Ranges	Accuracy
Temperature T_g	RTD sensor	0 ~ 200 °C	±0.12%
Temperatures T_e, T_c	RTD sensors	0 ~ 50 °C	±0.12%
Temperatures T_1-T_{11}	K-type thermocouples	−200 ~ 320 °C	±1.5 °C
Pressures P_g, P_e, P_c, P_{fp}	Industrial pressure gauges	−1 ~ 30 bar	±1.5%
Pressure P_{suc}	Bourdon-tube pressure gauge	−1 ~ 1 bar	±0.25%
Pressure P_c	Bourdon-tube pressure gauge	−1 ~ 2 bar	±0.25%
Refrigerant flow rates	Gear-type flow meters	0.1 ~ 6.0 l min^{-1}	±3.0%
Electric energy input	Electrical power meters	0 ~ 30 kW	±0.6%

nozzles were repeated 4–6 times to ensure that no variation occurred with the data taken from the generator heaters.

The primary flow was determined from the energy balance of the generator and it was also measured using a flow meter. The theoretical mass flow rate through the supersonic nozzle can be expressed by (Volovyk, 2013):

$$\dot{m}_p = A_t \cdot P_g \frac{\gamma}{\sqrt{\frac{2\cdot\gamma}{\gamma+1}\cdot\frac{P_g}{\rho_1}}} \cdot \left(\frac{2}{\gamma+1}\right)^{\frac{\gamma}{\gamma-1}} \cdot \upsilon \quad (8)$$

where γ is heat capacity ratio, and υ – stands for the flow coefficient.

The calculated values with flow coefficient $\upsilon = 0.95$ agree with the measured data perfectly.

4.2. *Experimental determination of optimal position of the nozzle*

During further research for all ejectors with cylindrical mixing chambers (CMC) several experiments were carried out which allowed to determine optimal distance l_n between exit cross-section of the nozzle and entrance cross-section of the mixing chamber. The nozzle was moved in the line of mixing chamber and the efficiency of the system was determined. Maximum entrainment ratio $\omega = \omega^{MAX}$ corresponds to this optimal position of the nozzle for design operating conditions.

Optimal values of l_n, which were received from the experiments, and the values of the main geometrical parameter of A_3/A_t for tested ejectors with CMC are shown in Table 6. All further researches, when the efficiency of the ejectors and ERM at design and off-design conditions was determined, were carried out at optimal values of the distance l_n.

4.3. *Experimental investigation of ejectors with cylindrical mixing chambers*

Once the supersonic nozzles were calibrated over a range of generating temperatures, the cooling machine was ready to conduct the full test for the designed ejector geometry over a range of design and off-design operating conditions.

The experimentation was carried out by varying the temperatures individually in the evaporator, condenser and generator. For each test the critical condensing temperature was established and determined.

Nine ejectors with cylindrical mixing chambers A, B and C were tested. The results of experimental investigations of ejectors with CMC operating at critical conditions are presented in Table 7.

Some typical of the test results obtained for the ejector cycle are shown in Fig. 11. These data were obtained for ejector 2-B with the area ratio $A_3/A_t = 9.55$ and optimal position of the nozzle $l_n = 20.6$ mm in the front of the entry section of the cylindrical mixing chamber.

An ejector 2-B with cylindrical mixing chamber using R245fa was designed for operation at $T_g = 95$ °C and $T_e = 12$ °C. Fig. 11 demonstrates the effect of the condensing temperature T_c on the ejector 2-B and ERM performance for evaporating temperatures T_e varying from 8 to 16 °C and $T_g = 95$ °C. For each given T_e, the entrainment ratio ω, thermal coefficient of performance COP_{therm} and cooling capacity Q_e are independent of the ejector back pressure, i.e., the condensing temperature and pressure. However, when the condensing temperature T_c is higher than a certain value, known as the "critical condensing temperature" T_c^*, then ω, COP_{therm} and Q_e will decrease suddenly and then fall to zero (Huang et al., 1985).

From obtained experimental results, it follows that the critical condensing temperature varies with generating and evaporating temperatures. This is therefore an important design criterion, which is determined by the highest temperature anticipated at the condenser heat sink. The optimum ejector and ERM performances can be obtained when the system operates at critical condensing temperatures. At a constant generating temperature, higher values of ω, COP_{therm} and Q_e can be achieved when the evaporating temperature is allowed to rise. Therefore, for air conditioning applications, it is preferable to design an ejector for high evaporating temperatures. This then leads the ERM to operate at higher critical condensing temperatures as the condenser heat sink temperature increases.

Figs. 12 and 13 illustrate the variations in theoretical trends and experimental critical values of A_3/A_t, ω^*, COP^*_{therm} and Q^*_e with T_e and T_c^* at $T_g = 95$ °C for ejectors 2-A, 2-B and 2-C.

It can be seen from Fig. 12 that theoretical $\alpha = A_3/A_t$ falls with increases in T_c^* and decreases in T_e. From Fig. 13 it follows that the theoretical characteristics ω^*, COP^*_{therm} and Q^*_e have the same trend: they increase with increment of T_e and decrement of T_c^*.

The theoretical results within experimental error are in good agreement with the corresponding experimental results.

In practice, the actual operating temperatures T_c, T_g and T_e vary with the surrounding conditions and usually are adjustable (Huang et al., 1985). A theoretical method for the determination of the optimal adjustment range subject to the requirements of the refrigeration user and concrete application conditions is given by Petrenko and Volovyk (2007). This method enables one to select the combination of three independent operating parameters T_e, T_c and T_g to provide maximum efficiency of the ERM at critical operating conditions.

The theoretical and experimental results were used to construct performance maps of all manufactured ejectors with cylindrical mixing chambers.

Fig. 14 shows the theoretical (dotted lines) and measured (solid lines) variations in ω^*, COP^*_{therm} and Q^*_e with the critical condensing temperatures over a range of evaporating and

Table 6 – Experimental values of A_3/A_t and l_n for tested ejectors.

Ejector	1-A	1-B	1-C	2-A	2-B	2-C	3-A	3-B	3-C
A_3/A_t	7.25	8.32	9.63	8.33	9.55	11.06	9.70	11.14	12.89
l_n, mm	16.4	19.3	22.8	16.2	20.6	24.2	20.5	22.9	26.3

Table 7 – Experimental data for the nominal (critical) conditions of tested ejectors with CMC.

Ejector	1-A	1-B	1-C	2-A	2-B	2-C	3-A	3-B	3-C
Generating temperature T_g, °C	90	90	90	95	95	95	100	100	100
Evaporating temperature T_e, °C	8	8	8	12	12	12	16	16	16
Critical condensing temperature T_c^*, °C	34.7	32.8	30.2	36.9	34.2	31.3	37.5	35.6	32.5
Critical entrainment ratio ω^*	0.241	0.318	0.402	0.345	0.423	0.536	0.471	0.575	0.744
Critical COP^*_{therm}	0.186	0.243	0.309	0.265	0.323	0.411	0.358	0.440	0.570
Critical cooling capacity Q_e^*, kW	3.1	4.1	5.2	4.4	5.4	7.0	5.7	7.0	9.2

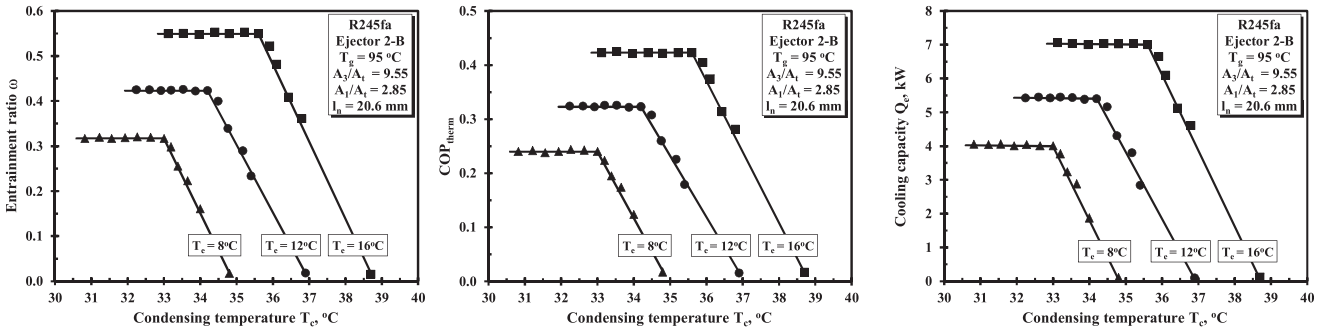

Fig. 11 – Measured variation in ω, COP_{therm} and Q_e with T_c at different T_e for ejector 2-B (with cylindrical mixing chamber).

generating temperatures for ejector 2-B. From Fig. 14 for experimental data, it follows that at the given adjustment range of T_e, which varied from 8 to 16 °C, in order to achieve the maximum performance of ERM with a variation of T_c^* in the range of 29.5–39.0 °C, the temperature T_g must also be adjusted in the range of 88.0–102.0 °C. Under these conditions, the characteristics ω^*, COP^*_{therm} and Q_e^* will take on various intermediate values in the following ranges: $\omega^* = 0.23–0.70$, $COP^*_{therm} = 0.17–0.55$ and $Q_e^* = 3.3–7.8$ kW.

Theoretical data show good coincidence with experimental results not only for the design points, but also for other off-design points. The maximum difference between the experimental results and the results of the proposed model falls within 5%.

The ERM performance maps provide useful assistance for the development of an automatic control system for the ERM operating at off-design operating conditions. Obtained test results demonstrate that solar energy or low-grade heat can be used to drive efficient ERMs operating with R245fa for air conditioning and space cooling.

The patterns described above were also determined for all other tested ejectors (Table 3).

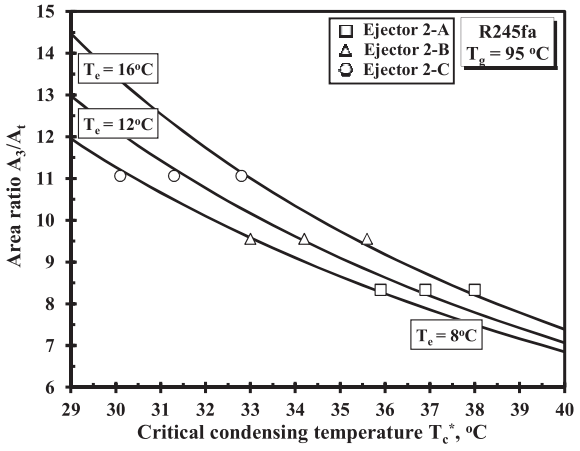

Fig. 12 – Variation in theoretical trends and experimental values of A_3/A_t with T_e and T_c^* at $T_g = 95$ °C for different ejectors.

4.4. *Experimental investigation of ejectors with conical-cylindrical mixing chambers*

Furthermore, nine ejectors with conical-cylindrical mixing chambers (CCMC) were also tested at the same operating conditions. The results of experimental investigations of ejectors with CCMC operating at critical conditions are presented in Table 8.

Geometrical characteristics A_3/A_t of tested ejectors with CCMC were the same as for ejectors with CMC, and for all ejectors with CCMC the value of $\beta = 1.3$. Some typical test results obtained for the ejector 2–2 with area ratio $A_3/A_t = 9.55$ and optimal position of the nozzle $l_n = 20.6$ mm are shown in Fig. 15.

From Fig. 15 it can be seen that at $T_g = 88$, 95 and 102 °C and $T_e = 12$ °C the behavior of $\omega = f(T_c)$, $COP_{therm} = f(T_c)$ and $Q_e = f(T_c)$ for ejector 2–2 with CCMC is the same as similar functions for ejector 2-B with CMC. For ejector 2–2 it can be found that the values of ω, COP_{therm} and Q_e are higher and T_c^* are lower compared to ejector 2-B.

The comparison of ω^*, COP^*_{therm} and Q_e^* for ejectors with nozzle 2 between cylindrical and conical-cylindrical mixing chambers at design operating conditions (see Fig. 16) shows that the application of the conical-cylindrical mixing chambers throughout considered range of critical condensing temperatures $T_c^* = 31.3–35.6$ °C allows for the increasing of ejector and ERM efficiency up to 20% on the average.

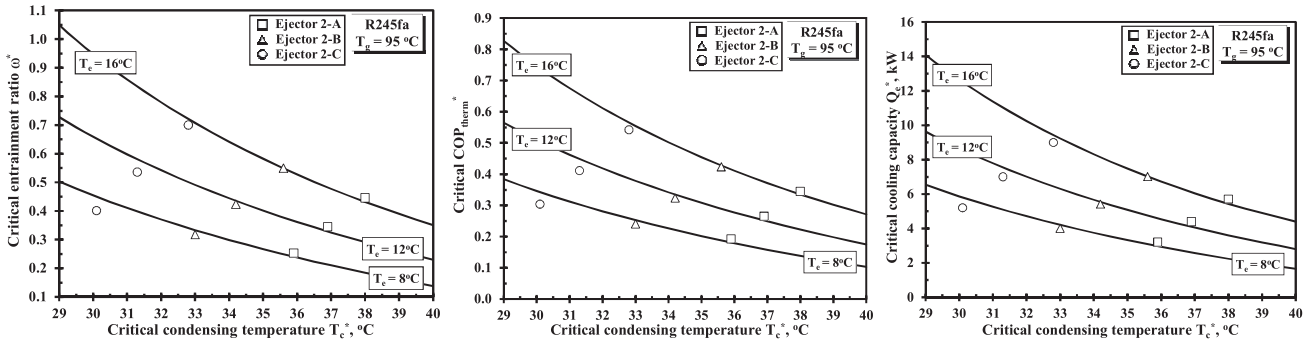

Fig. 13 – – Variation in theoretical trends and experimental critical values of ω^*, COP^*_{therm} and Q^*_e with T_e and T^*_c at $T_g = 95$ °C for different ejectors.

Fig. 17 shows the efficiency of ejector 2–2 in a form of performance maps, which were constructed from the theoretical and experimental results to show the ejector performance characteristics, from which the design analysis of ejector refrigeration system could be carried out.

The efficiency comparison of ejector with cylindrical and conical-cylindrical mixing chambers is made. The results of this comparison are shown in Fig. 18.

Average improvement in efficiency of ejectors with CCMC over ejectors with CMC is in the range from 23.5%: from 15% for ejector 3–1 compared to 3-A up to 54% for ejector 1–1 compared to 1-A. The critical condensing temperature T^*_c decreases 1.2–1.6 °C for ejectors with CCMC because their main geometrical characteristic A_3/A_t remained the same as for ejectors with CMC. The relative increasing in entrainment ratio corresponds to the higher condensing temperatures; this means that the application of CCMC is more preferable for high condensing temperatures.

The generating temperature for each compared ejectors was the same, resulting in similar flow core at the exit of the nozzle. Ejectors with conical-cylindrical mixing chambers had conical part of the mixing chamber at the entrance. This leads to the increase in flow area for entrained refrigerant vapor (increasing of entrainment ratio). But the diameter of the cylindrical part of the mixing chamber was the same as well as the other geometry. It means that the energy of the primary working stream was not enough to compress larger (compared to CMC) amount of entrained vapor up to the pressure corresponding to the critical condensing pressure obtained for ejectors with CMC. That's why the critical condensing temperature for ejectors with CCMC was lower. In order to equalize the critical condensing temperatures for such ejectors it is necessary to make smaller diameter of cylindrical part of mixing chamber of ejector with CCMC. But in the presented research the authors changed only one geometrical parameter.

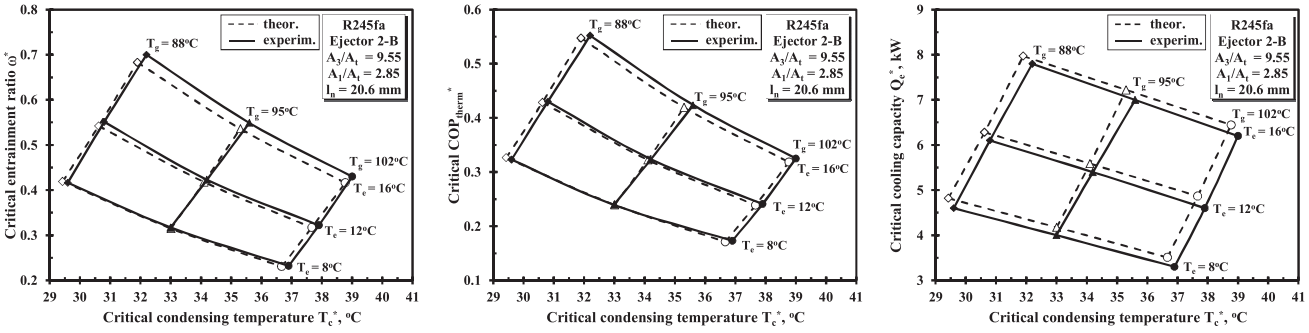

Fig. 14 – Measured and theoretical variation in ω^*, COP^*_{therm} and Q^*_e with T_c^* over a range of T_e and T_g for ejector 2-B (with cylindrical mixing chamber).

Table 8 – Experimental data for the nominal (critical) conditions of tested ejectors with CCMC.

Ejector	1–1	1–2	1–3	2–1	2–2	2–3	3–1	3–2	3–3
Generating temperature T_g, °C	90	90	90	95	95	95	100	100	100
Evaporating temperature T_e, °C	8	8	8	12	12	12	16	16	16
Critical condensing temperature T^*_c, °C	34.7	31.7	29.0	35.6	33.0	29.7	36.7	33.9	30.8
Critical entrainment ratio ω^*	0.355	0.437	0.529	0.449	0.544	0.673	0.587	0.727	0.892
Critical COP^*_{therm}	0.270	0.334	0.407	0.340	0.413	0.516	0.447	0.556	0.689
Critical cooling capacity Q^*_e, kW	4.5	5.6	7.1	5.6	6.8	8.7	7.0	8.9	11.4

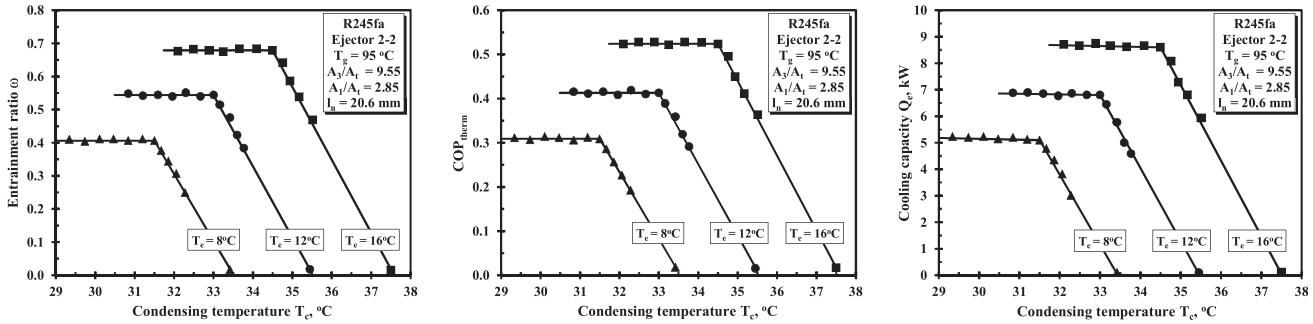

Fig. 15 – Measured variation in ω, COP_{therm} and Q_e with T_c at different T_e for ejector 2–2 (with conical-cylindrical mixing chamber).

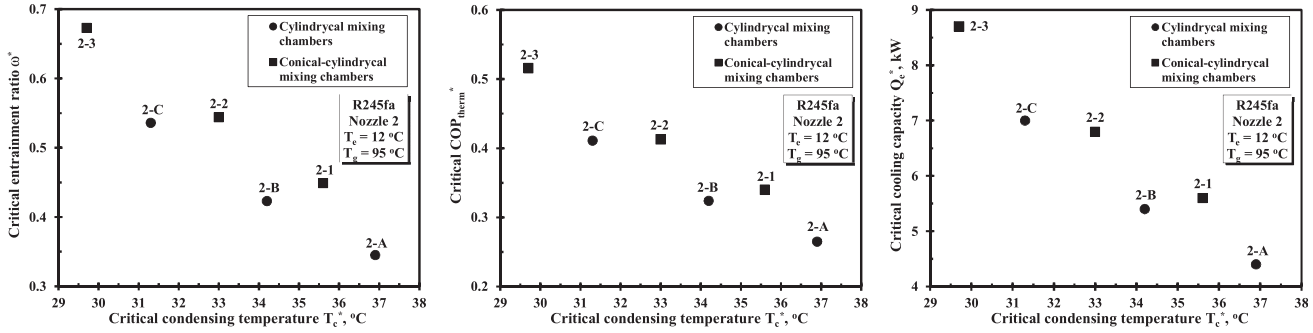

Fig. 16 – Comparison of ω^*, COP^*_{therm} and Q^*_e for design working conditions at T_e = 12 °C and T_g = 95 °C.

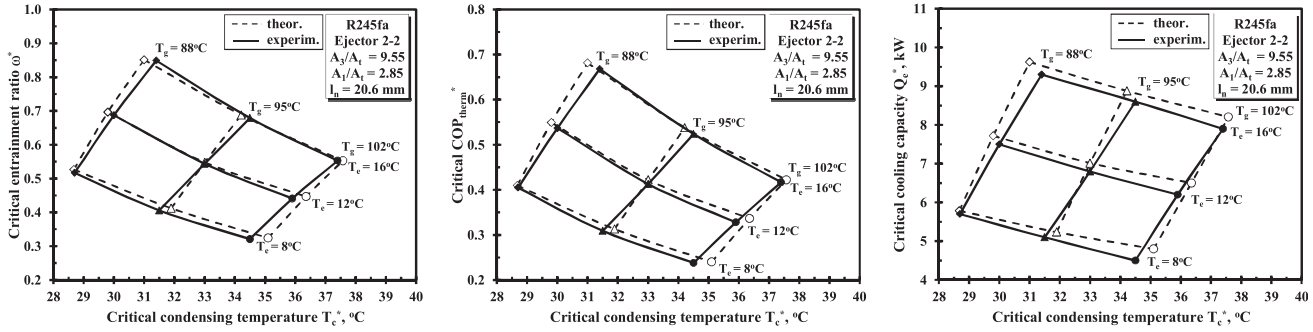

Fig. 17 – Measured and theoretical variation in ω^*, COP^*_{therm} and Q^*_e with T_c* over a range of T_e and T_g for ejector 2–2 (with conical-cylindrical mixing chamber).

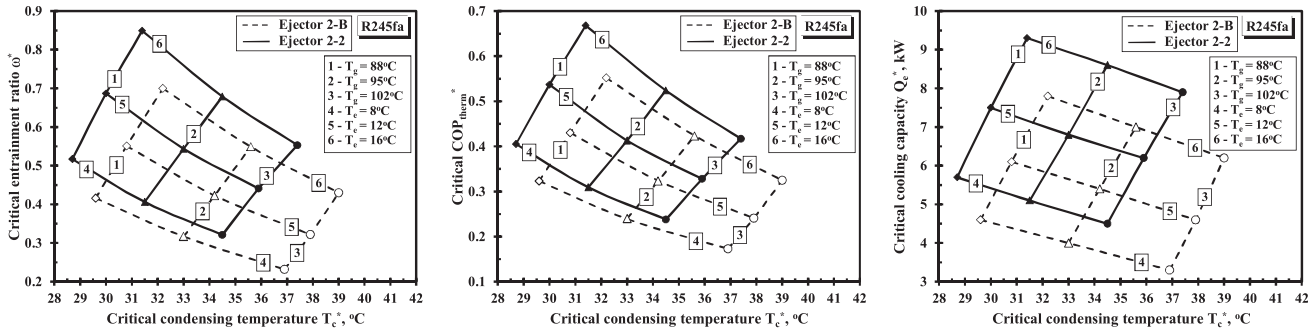

Fig. 18 – Measured variation in ω^*, COP^*_{therm} and Q^*_e with T_c* over a range of T_e and T_g for ejectors 2-B and 2–2.

5. Conclusions

The testing technique for the experimental investigation of ERM with maximum cooling capacity of 12.0 kW operating at design and off-design conditions is presented. The described testing technique is proposed to carry out the assessment of the suggested ERM. The main components of the system are specially designed and the instrumentation generally is classic for refrigeration test rig.

This paper presents the results of a theoretical and experimental investigation of an ejector and ejector refrigeration machine operating with refrigerant R245fa.

The effect of the ejector cycle operating conditions on the ejector and ERM performance characteristics is studied in this part. A comparison of the test results and the model predictions demonstrates that the experimental performances at the design operating conditions are about 10% higher than the theoretical values. The main reason for this is that the advanced experimental ejector has lower process irreversibility and energy loss than was assumed in 1-D model.

The obtained test results demonstrate that low-grade heat or solar energy can be used to drive efficient ERMs operating with R245fa and designed for air conditioning and space cooling.

Acknowledgments

This publication is based on the work supported by Award No.KUK-C1-014-12, made by King Abdullah University of Science and Technology (KAUST), Saudi Arabia.

REFERENCES

Eames, I.W., Ablwaifa, A.E., Petrenko, V.O., 2007. Results of an experimental study of an advanced jet-pump refrigerator operating with R245fa. Appl. Therm. Eng. 27, 2833–2840.

Eames, I.W., Petrenko, V.O., Ablwaifa, A.E., 2004. Design and experimental investigation of a jet pump refrigerator. In: Proc. 3rd International Conference on Heat Powered Cycles, HPC (Larnaca, Cyprus).

Huang, B.J., Jiang, C.B., Hu, F.L., 1985. Ejector performance characteristics and design analysis of jet refrigeration system. J. Eng. Gas Turb. Power 107, 792–802.

Huang, B.J., Chang, J.M., Wang, C.P., Petrenko, V.O., 1999. A 1-D analysis of ejector performance. Int. J. Refrigeration 22 (5), 354–364.

Petrenko, V.O., Volovyk, O.S., 2007. Analysis of performance characteristics of ejector refrigeration machine operating at design and off-design conditions. Refrig. Eng. Technol. 2 (106), 20–26.

Petrenko, V.O., Huang, B.J., Shestopalov, K.O., Ierin, V.O., Volovyk, O.S., 2011. An advanced solar-assisted cascade ejector cooling/CO_2 sub-critical mechanical compression refrigeration system. In: ISES Solar World Congress 2011, 28 August – 2 September, Kassel, Germany.

Petrenko, V.O., 1978. Investigation of Ejector Cooling Machine Operating with Refrigerant R142b. Odessa Technological Institute of Refrigeration Industry, Ukraine. Ph.D. thesis.

Shestopalov, K.O., Huang, B.J., Petrenko, V.O., Volovyk, O.S., 2015. Investigation of an experimental ejector refrigeration machine operating with refrigerant R245fa at design and off-design working conditions. Part 1. Theoretical analysis. Int. J. Refrigeration.

Volovyk, O.S., 2013. Improvement of Characteristics and Performances of an Ejector Refrigeration Machine Operating with Low-boiling Working Fluids. Odessa National Academy of Food Technologies, Ukraine. Ph.D. thesis.